Energy Transfer Followed by Electron Transfer in a Supramolecular Triad Composed of Boron Dipyrrin, Zinc Porphyrin, and Fullerene: A Model for the Photosynthetic Antenna-Reaction Center Complex

Francis D'Souza,*,[†] Phillip M. Smith,[†] Melvin E. Zandler,[†] Amy L. McCarty,[†]
Mitsunari Itou,[‡] Yasuyuki Araki,[‡] and Osamu Ito*,[‡]

*Contribution from the Department of Chemistry, Wichita State University,
1845 Fairmount, Wichita, Kansas 67260-0051, and Institute of Multidisciplinary Research for
Advanced Materials, Tohoku University, Katahira, Sendai, 980-8577, Japan*

Received December 3, 2003; Revised Manuscript Received April 12, 2004; E-mail: francis.dsouza@wichita.edu; ito@tagen.tohoku.ac.jp

Abstract: The first example of a working model of the photosynthetic antenna-reaction center complex, constructed via self-assembled supramolecular methodology, is reported. For this, a supramolecular triad is assembled by axially coordinating imidazole-appended fulleropyrrolidine to the zinc center of a covalently linked zinc porphyrin−boron dipyrrin dyad. Selective excitation of the boron dipyrrin moiety in the boron dipyrrin−zinc porphyrin dyad resulted in efficient energy transfer ($k_{ENT}^{singlet} = 9.2 \times 10^9$ s^{-1}; $\Phi_{ENT}^{singlet} = 0.83$) creating singlet excited zinc porphyrin. Upon forming the supramolecular triad, the excited zinc porphyrin resulted in efficient electron transfer to the coordinated fullerenes, resulting in a charge-separated state ($k_{cs}^{singlet} = 4.7 \times 10^9$ s^{-1}; $\Phi_{CS}^{singlet} = 0.9$). The observed energy transfer followed by electron transfer in the present supramolecular triad mimics the events of natural photosynthesis. Here, the boron dipyrrin acts as antenna chlorophyll that absorbs light energy and transports spatially to the photosynthetic reaction center, while the electron transfer from the excited zinc porphyrin to fullerene mimics the primary events of the reaction center where conversion of the electronic excitation energy to chemical energy in the form of charge separation takes place. The important feature of the present model system is its relative "simplicity" because of the utilized supramolecular approach to mimic rather complex "combined antenna-reaction center" events of photosynthesis.

Introduction

Photosynthesis, the process of converting light energy into chemical energy, involves two major steps, absorption and transportation of light energy of appropriate wavelength by the antenna light harvesting molecules to the reaction center, and photoinduced electron transfer (PET) to generate charge-separated entities by using the electronic excitation energy.[1] The light energy harvesting antenna system consists of chromophore arrays which transport energy via a mechanism of singlet−singlet energy transfer among the chromophores. These antenna chromophores vary from organism to organism and are optimized for the quality of light in a particular environment and are effectively coupled to the reaction center. The reaction center absorbs the excitation energy and converts it to chemical energy in the form of transmembrane charge separation via a multistep electron-transfer reaction. The stored energy in the form of

charge-separated species (electrochemical energy) is later converted into other forms of biologically useful energy such as proton motive force.[1]

Mimicking the photosynthetic functions by using synthetic model compounds is important to further our understanding of the process of bioenergetics. Research in this area also holds promise for technological advances in solar energy conversion, and building molecular optoelectronics such as photonic wires and switches. In this regard, several studies on artificial photosynthesis focused on PET, and many reaction center mimicking compounds have been synthesized and studied.[2−9]

[†] Wichita State University.
[‡] Tohoku University.
(1) (a) Barber, J.; Anderson, B. *Nature* **199**4, *370*, 31. (b) El-Kobbani, O.; Chang, C. H.; Tiede, D.; Norris, J.; Schiffer, M. *Biochemistry* **1991**, *30*, 5361. (c) Fromme, P. *Curr. Opin. Struct. Biol.* **1996**, *6*, 473. (d) Krauss, N.; Schubert, W. D.; Klukas, O.; Fromme, P.; Witt, H. T.; Saenger, W. *Nat. Struct. Biol.* **1996**, *3*, 965. (e) Nugent, J. H. A. *Eur. J. Biochem.* **1996**, *237*, 519. (f) *The Photosynthetic Reaction Center*; Deisenhofer, J., Norris, J. R., Eds.; Academic Press: San Diego, 1993. (g) Deisenhofer, J.; Epp, O.; Miki, K.; Huber, R.; Michel, H. *J. Mol. Biol.* **1984**, *180*, 385.

(2) (a) Connolly, J. S., Ed. *Photochemical Conversion and Storage of Solar Energy*; Academic: New York, 1981. (b) Wasielewski, M. R. *Chem. Rev.* **1992**, *92*, 435. (c) Jordan, K. D.; Paddon-Row, M. N. *Chem. Rev.* **1992**, *92*, 395. (d) Verhoeven, J. W. *Adv. Chem. Phys.* **1999**, *106*, 603. (e) Osuka, A.; Mataga, N.; Okada, T. *Pure Appl. Chem.* **1997**, *69*, 797. (f) Flamigni, L.; Barigelletti, F.; Armaroli, N.; Collin, J.-P.; Dixon, I. M.; Sauvage, J.-P.; Williams, J. A. G. *Coord. Chem. Rev.* **1999**, *190−192*, 671. (g) Diederich, F.; Gomez-Lopez, M. *Chem. Rev. Soc.* **1999**, *28*, 263.
(3) (a) Blanco, M.-J.; Consuelo Jimenez, M.; Chambron, J.-C.; Heitz, V.; Linke, M.; Sauvage, J.-P. *Chem. Rev. Soc.* **1999**, *28*, 293. (b) Campagna, S.; Di Pietro, C.; Loiseau, F.; Maubert, B.; McClenaghan, N.; Passalacqua, R.; Puntoriero, F.; Ricevuto, V.; Serroni, S. *Coord. Chem. Rev.* **2002**, *229*, 67. (c) Balzani, V.; Ceroni, P.; Juris, A.; Venturi, M.; Campagna, S.; Puntoriero, F.; Serroni, S. *Coord. Chem. Rev.* **2001**, *219*, 545.
(4) (a) Bixon, M.; Fajer, J.; Feher, G.; Freed, J. H.; Gamliel, D.; Hoff, A. J.; Levanon, H.; Möbius, K.; Nechushtai, R.; Norris, J. R.; Scherz, A.; Sessler, J. L.; Stehlik, D. *Isr. J. Chem.* **1992**, *32*, 449. (b) Lewis, F. D.; Letsinger, R. L.; Wasielewski, M. R. *Acc. Chem. Res.* **2001**, *34*, 159.

The majority of these compounds are based on porphyrin chromophores linked to one or more electron donor or acceptor molecules. The efficiency and quantum yield of charge separation in some of these systems were comparable to those found in natural reaction centers. To mimic the antenna function, singlet energy transfer between two or more covalently linked or self-assembled porphyrins, or other chromophores, has been studied extensively.[10–16] Some of these molecular/supramolecular systems have revealed potential for constructing photonic, electronic, and optoelectronic devices.[17,18]

Developing an artificial light harvesting system with a reaction center mimic to produce a complex capable of absorbing light, transferring the resulting excitation to an energy sink, and using the captured energy to initiate PET is one of the major advancements in this area of research. A few elegantly designed molecular systems involving covalently linked zinc porphyrin(s), free-base porphyrin(s), and fullerene have been

Scheme 1
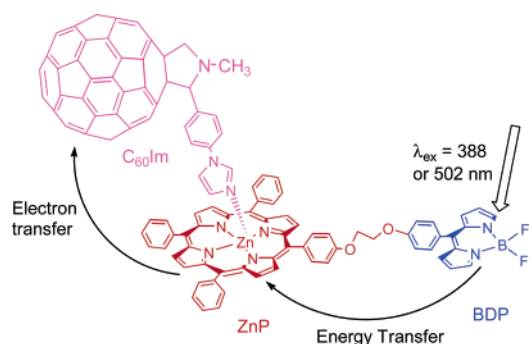
synthesized and studied.[13,19–21] Our aim here is to employ a supramolecular approach to develop such a combined antenna-reaction center model system (Scheme 1) and to study sequential energy- and electron-transfer events. In Scheme 1, boron dipyrrin (BDP) acts as an energy absorbing and transferring antenna, and zinc porphyrin (ZnP) acts as an energy acceptor from the antenna and promotes electron transfer to the fullerene moiety by using the excitation energy, with the fullerene (C_{60}-Im) being the electron acceptor. We have selected the BDP–ZnP dyad for the initial energy transfer because of (i) the excitation wavelength selectivity; that is, when the molecule is excited either at 388 or at 480–505 nm light, only the BDP of the dyad is excited, leaving the ZnP in the ground state;[22] and (ii) the ZnP can bind an electron acceptor entity via metal–ligand coordination to form a supramolecular triad.[23a] Fullerene, C_{60}, is the choice of electron acceptor because of its low reorganization energy in electron-transfer reactions.[23b–d] We have selected an imidazole-appended fulleropyrrolidine, C_{60}-Im, as a ligand bearing electron acceptor to axially coordinate to ZnP, because our recent studies have shown that the C_{60}Im binds to ZnP better than C_{60} bearing other coordinating ligand such as pyridine.[24] Because of the higher stability of the self-assembled ZnP–C_{60}Im dyad, the magnitude of the rate and quantum yield of PET was comparable to that observed for covalently linked ZnP–C_{60} dyads.[24]

Results and Discussion

Ground-State Properties of the Boron Dipyrrin–Zinc Porphyrin Dyad. The synthesis of boron dipyrrin–zinc porphyrin dyad employed in the present study involved first preparation of dipyrromethane using pyrrole and 4-bromoethoxybenzaldehyde followed by conversion of the dipyrromethane to boron dipyrrin. The functionalized boron dipyrrin

(5) (a) Gust, D.; Moore, T. A.; Moore, A. L. *Acc. Chem. Res.* **1993**, *26*, 198. (b) Gust, D.; Moore, T. A. In *The Porphyrin Handbook*; Kadish, K. M., Smith, K., Guilard, R., Eds.; Academic Press: San Diego, 2000; Vol. 8, pp 153–190.

(6) (a) Fukuzumi, S.; Guldi, D. M. In *Electron Transfer in Chemistry*; Balzani, V., Ed.; Wiley-VCH: Weinheim, 2001; Vol. 2, pp 270–337. (b) Fukuzumi, S. In *The Porphyrin Handbook*; Kadish, K. M., Smith, K., Guilard, R., Eds.; Academic Press: San Diego, 2000; Vol. 8, pp 115–151.

(7) (a) Sakata, Y.; Imahori, H.; Tsue, H.; Higashida, S.; Akiyama, T.; Yoshizawa, E.; Aoki, M.; Yamada, K.; Hagiwara, K.; Taniguchi, S.; Okada, T. *Pure Appl. Chem.* **1997**, *69*, 1951. (b) Imahori, H.; Sakata, Y. *Eur. J. Org. Chem.* **1999**, 2445. (c) Imahori, H.; Tamaki, K.; Araki, Y.; Sekiguchi, Y.; Ito, O.; Sakata, Y.; Fukuzumi, S. *J. Am. Chem. Soc.* **2002**, *124*, 5165. (d) Asahi, T.; Ohkouchi, M.; Matsusaka, R.; Mataga, N.; Zhang, R. P.; Osuka, A.; Maruyama, K. *J. Am. Chem. Soc.* **1993**, *115*, 5665.

(8) (a) Guldi, D. M. *Chem. Commun.* **2000**, 321. (b) Guldi, D. M. *Chem. Soc. Rev.* **2002**, *31*, 22.

(9) (a) Ward, M. W. *Chem. Soc. Rev.* **1997**, *26*, 365. (b) Hayashi, T.; Ogoshi, H. *Chem. Soc. Rev.* **1997**, *26*, 355. (c) Sessler, J. S.; Wang, B.; Springs, S. L.; Brown, C. T. In *Comprehensive Supramolecular Chemistry*; Atwood, J. L., Davies, J. E. D., MacNicol, D. D., Vögtle, F., Eds.; Pergamon: New York, 1996; Chapter 9.

(10) Seth, J.; Palaniappan, V.; Johnson, T. E.; Prathapan, S.; Lindsey, J. S.; Bocian, D. F. *J. Am. Chem. Soc.* **1994**, *116*, 10578.

(11) (a) Seth, J.; Palaniappna, V.; Wagner, R. W.; Johnson, T. E.; Lindsey, J. S.; Holten, D.; Bocian, D. F. *J. Am. Chem. Soc.* **1996**, *118*, 11194. (b) Hsiao, J.-S.; Krueger, B. J.; Wagner, R. W.; Johnson, T. E.; Delaney, J. K.; Mauzerall, D. C.; Fleming, G. R.; Lindsey, J. S.; Bocian, D. F.; Donohoe, R. J. *J. Am. Chem. Soc.* **1996**, *118*, 11181.

(12) (a) Sessler, J. L.; Magda, D. J.; Harriman, A. *J. Am. Chem. Soc.* **1995**, *117*, 704. (b) Kral, V.; Springs, S. L.; Sessler, J. L. *J. Am. Chem. Soc.* **1995**, *117*, 8881. (c) Springs, S. L.; Gosztola, D.; Wasielewski, M. R.; Kral, V.; Andrievsky, A.; Sessler, J. L. *J. Am. Chem. Soc.* **1999**, *121*, 2281. (d) Bothner-By, A. A.; Dodok, J.; Johnson, T. E.; Delaney, J. K.; Lindsey, J. S. *J. Phys. Chem.* **1996**, *100*, 17551.

(13) Luo, C.; Guldi, D. M.; Imahori, H.; Tamaki, K.; Sakata, Y. *J. Am. Chem. Soc.* **2000**, *122*, 6535.

(14) (a) Wagner, R. W.; Johnson, T. E.; Lindsey, J. S. *J. Am. Chem. Soc.* **1996**, *118*, 11166. (b) Strachan, J. P.; Gentemann, S.; Seth, J.; Kalsback, W. A.; Lindsey, J. S.; Holten, D.; Bocian, D. F. *J. Am. Chem. Soc.* **1997**, *119*, 11191. (c) Li, F.; Gentemann, S.; Kalsbeck, W. A.; Seth, J.; Lindsey, J. S.; Holten, D.; Bocian, D. F. *J. Mater. Chem.* **1997**, *7*, 1245.

(15) (a) Giribabu, L.; Kumar, A.; Neeraja, V.; Maiya, B. G. *Angew. Chem., Int. Ed.* **2001**, *40*, 3621. (b) Aratani, N.; Cho, H. S.; Ahn, T. K.; Cho, S.; Kim, D.; Sumi, H.; Osuka, A. *J. Am. Chem. Soc.* **2003**, *125*, 9668. (c) Shinmori, H.; Ahn, T. K.; Cho, H. S.; Kim, D.; Yoshida, N.; Osuka, A. *Angew. Chem., Int. Ed.* **2003**, *42*, 2754. (d) Choi, M.-S.; Aida, T.; Yamazaki, T.; Yamazaki, I. *Chem.-Eur. J.* **2002**, *8*, 2667. (e) Choi, M.-S.; Aida, T.; Luo, H.; Araki, Y.; Ito, O. *Angew. Chem., Int. Ed.* **2003**, *42*, 4060.

(16) (a) Splan, K. E.; Keefe, M. H.; Massari, A. M.; Walters, K. A.; Hupp, J. T. *Inorg. Chem.* **2002**, *41*, 619. (b) Nakano, A.; Yasuda, Y.; Yamazaki, T.; Akimoto, S.; Yamazaki, I.; Miyasaka, H.; Itaya, A.; Murakami, M.; Osuka, A. *J. Phys. Chem. A* **2001**, *105*, 4822.

(17) (a) Wagner, R. W.; Lindsey, J. S. *J. Am. Chem. Soc.* **1994**, *116*, 9759. (b) Wagner, R. W.; Lindsey, J. S.; Seth, J.; Palaniappna, V.; Bocian, D. F. *J. Am. Chem. Soc.* **1996**, *118*, 3996. (c) Abbroise, A.; Wagner, R. W.; Rao, P. D.; Riggs, J. A.; Hascoat, P.; Diers, J. R.; Seth, L.; Robin, K.; Bocian, D. F.; Holten, D.; Lindsey, J. S. *Chem. Mater.* **2001**, *13*, 1023. (d) Ambroise, A.; Kirmaier, C.; Wagner, R. W.; Loewe, R. S.; Bocian, D. F.; Holten, D.; Lindsey, J. S. *J. Org. Chem.* **2002**, *67*, 3811.

(18) (a) *Introduction of Molecular Electronics*; Petty, M. C., Bryce, M. R., Bloor, D., Eds.; Oxford University Press: New York, 1995. Balzani, V.; Credi, A.; Raymo, F. M.; Stoddart, J. F. *Angew. Chem., Int. Ed.* **2000**, *39*, 3348. (b) Belser, P.; Bernhard, S.; Blum, C.; Beyeler, A.; De Cola, L.; Balzani, V. *Coord. Chem. Rev.* **1999**, *190–192*, 155. (c) Carroll, R. L.; Gorman, C. R. *Angew. Chem., Int. Ed.* **2002**, *41*, 4378.

(19) Kuciauskas, D.; Liddell, P. A.; Lin, S.; Johnson, T. E.; Weghorn, S. J.; Lindsey, J. S.; Moore, A. L.; Moore, T. A.; Gust, D. *J. Am. Chem. Soc.* **1999**, *121*, 8604.

(20) Kodis, G.; Liddell, P. A.; de la Garza, L.; Clausen, C.; Lindsey, J. S.; Moore, A. L.; Moore, T. A.; Gust, D. *J. Phys. Chem. A* **2002**, *106*, 2036.

(21) Tamaki, K.; Imahori, H.; Nishimura, Y.; Yamazaki, I.; Sakata, Y. *Chem. Commun.* **1999**, 625.

(22) Li, F.; Yang, S. I.; Ciringh, T.; Seth, J.; Martin, C. H., III; Singh, D. L.; Kim, D.; Birge, R. R.; Bocian, D. F.; Holten, D.; Lindsey, J. S. *J. Am. Chem. Soc.* **1998**, *120*, 10001.

(23) (a) D'Souza, F.; Rath, N. P.; Deviprasad, G. R.; Zandler, M. E. *Chem. Commun.* **2001**, 267. (b) Imahori, H.; Mori, Y.; Matano. *J. Photochem. Photobiol., C: Photochem. Rev.* **2003**, *4*, 51. (c) Fukuzumi, S.; Imahori, H.; Yamada, H.; El-Khouly, M. E.; Fujitsuka, M.; Ito, O.; Guldi, D. M. *J. Am. Chem. Soc.* **2001**, *123*, 2571. (d) Fukuzumi, S.; Imahori, H.; Okamoto, K.; Yamada, H.; Fujitsuka, M.; Ito, O.; Guldi, D. M. *J. Phys. Chem. A* **2002**, *106*, 1903.

(24) D'Souza, F.; Deviprasad, G. R.; Zandler, M. E.; Hoang, V. T.; Arkady, K.; VanStipdonk, M.; Perera, A.; El-Khouly, M. E.; Fujitsuka, M.; Ito, O. *J. Phys. Chem. A* **2002**, *106*, 3243.
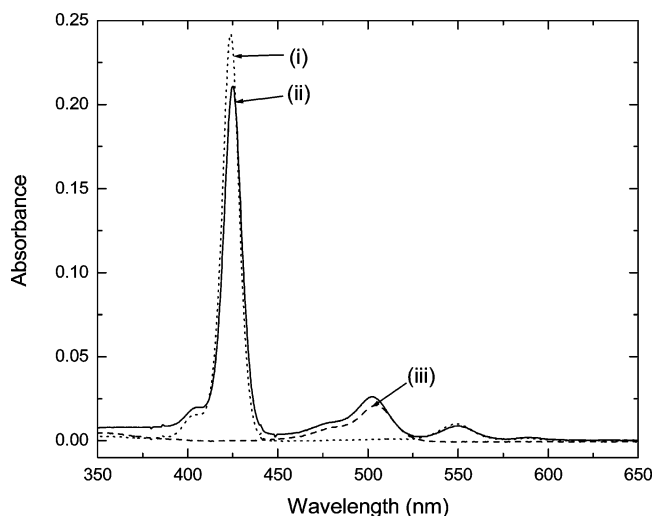
Figure 1. Steady-state absorption spectra of (i) zinc tetraphenylporphyrin (ZnP), (ii) ZnP−BDP dyad, and (iii) *meso*-phenyl boron dipyrrin (BDP) in *o*-dichlorobenzene. The concentrations were held at 0.4 μM.

was linked to 4-hydroxyphenyl-derivatized free-base porphyrin which was subsequently converted into its zinc derivative. Figure 1 shows the optical absorption spectrum of the boron dipyrrin−zinc porphyrin dyad along with reference compounds, *meso*-phenyl boron dipyrrin, and zinc tetraphenylporphyrin (ZnP) in *o*-dichlorobenzene. The absorption bands of the dyad located at 425, 502, 552, and 593 nm were shifted by 1−2 nm as compared to those of the pristine ZnP and phenyl boron dipyrrin, indicating some ground-state interactions between the two chromophores. Importantly, the weak absorption of boron dipyrrin at 360 nm and the stronger absorption at 502 nm had no overlap with the ZnP absorption at these wavelengths. Hence, irradiation of the dyad at either of these wavelengths is expected to selectively excite the boron dipyrrin moiety of the dyad.

Electrochemical studies using the cyclic voltammetric technique were performed to arrive at the redox potentials of the investigated compounds. Boron dipyrrin exhibited a reversible one-electron reduction at $E_{1/2} = -1.33$ V vs Fc/Fc$^+$ in *o*-dichlorobenzene. Additional irreversible redox waves at $E_{pc} = -2.38$ V and $E_{pa} = 1.48$ V vs Fc/Fc$^+$ were also observed under the experimental conditions (Figure 2a). In the dyad, the first reduction of boron dipyrrin was located at $E_{1/2} = -1.35$ V vs Fc/Fc$^+$ along with another reduction wave corresponding to the reduction of the zinc porphyrin moiety at $E_{1/2} = -1.95$ V vs Fc/Fc$^+$. Two one-electron reversible processes at $E_{1/2} = 0.26$ and 0.57 V vs Fc/Fc$^+$ were also observed, corresponding to the oxidations of the zinc porphyrin moiety (Figure 2b). Scanning the potential to more negative and positive potentials revealed additional irreversible waves of boron dipyrrin reduction and oxidations, similar to those observed for the reference compound. Under similar solution conditions, the imidazole bearing fulleropyrrolidine revealed three reductions at $E_{1/2} = -1.13$, -1.51, and -2.05 V vs Fc/Fc$^+$ (Figure 2c). From these electrochemical data on adding the excited energies and distances between the chromophores (vide infra), the free energies of charge separation (ΔG_{CS}) and charge recombination (ΔG_{CR}) were calculated using the Weller equation[25] as listed in Table 1.

(25) Weller, A. Z. *Phys. Chem.* **1982**, *132*, 93.
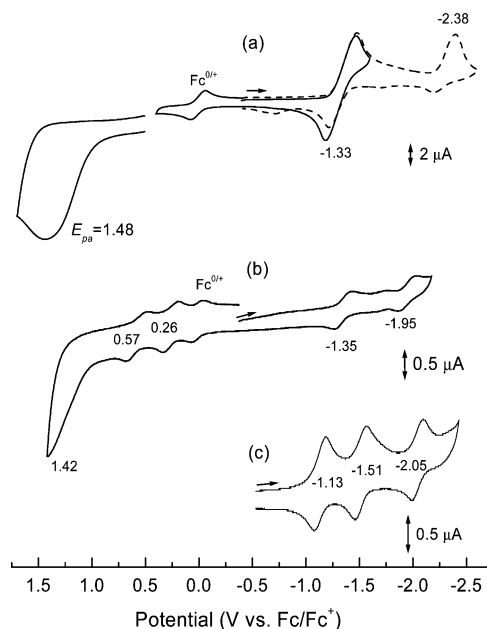
Figure 2. Cyclic voltammograms of (a) BDP, (b) ZnP−BDP dyad, and (c) imidazole-appended fulleropyrrolidine (C$_{60}$Im) in *o*-dichlorobenzene, 0.1 M (TBA)ClO$_4$. Scan rate = 100 mV/s.

An examination of the reduction potentials of the different moieties in the present study reveals that the boron dipyrrin is more difficult to reduce by 220 mV as compared to the first reduction of fulleropyrrolidine. That is, fulleropyrrolidine is a better electron acceptor than boron dipyrrin. However, the reduction potential of boron dipyrrin is comparable to those of methyl naphthaquinone or duroquinone, which are good electron acceptors from the singlet excited zinc porphyrin.[26] These results suggest that the boron dipyrrin could be an electron acceptor from the singlet excited zinc porphyrin in the dyad. To visualize this property, computational studies were performed using density functional methods (DFT) at the B3LYP/3-21G(*) level.[27] The DFT method over the Hartree−Fock or semiempirical approaches is chosen because recent studies have shown that the DFT-B3LYP methods at the 3-21G(*) level predict the geometry and electronic structure more accurately.[28] For this study, the dyad was fully optimized to a stationary point on the Born−Oppenheimer potential energy surface (Figure 3), and an ultrafine integration grid was used.

(26) D'Souza, F. *J. Am. Chem. Soc.* **1996**, *118*, 923.
(27) Frisch, M. J.; Trucks, G. W.; Schlegel, H. B.; Scuseria, G. E.; Robb, M. A.; Cheeseman, J. R.; Zakrzewski, V. G.; Montgomery, J. A.; Stratmann, R. E.; Burant, J. C.; Dapprich, S.; Millam, J. M.; Daniels, A. D.; Kudin, K. N.; Strain, M. C.; Farkas, O.; Tomasi, J.; Barone, V.; Cossi, M.; Cammi, R.; Mennucci, B.; Pomelli, C.; Adamo, C.; Clifford, S.; Ochterski, J.; Petersson, G. A.; Ayala, P. Y.; Cui, Q.; Morokuma, K.; Malick, D. K.; Rabuck, A. D.; Raghavachari, K.; Foresman, J. B.; Cioslowski, J.; Ortiz, J. V.; Stefanov, B. B.; Liu, G.; Liashenko, A.; Piskorz, P.; Komaromi, I.; Gomperts, R.; Martin, R. L.; Fox, D. J.; Keith, T.; Al-Laham, M. A.; Peng, C. Y.; Nanayakkara, A.; Gonzalez, C.; Challacombe, M.; Gill, P. M. W.; Johnson, B. G.; Chen, W.; Wong, M. W.; Andres, J. L.; Head-Gordon, M.; Replogle, E. S.; Pople, J. A. *Gaussian 98*, revision A.9; Gaussian, Inc.: Pittsburgh, PA, 1998.
(28) (a) Brown, S. T.; Rienstra-Kiracofe, J. C.; Schaefer, H. F. *J. Phys. Chem. A* **1999**, *103*, 4065−4077. (b) Rienstra-Kiracofe, J. C.; Barden, C. J.; Brown, S. T.; Schaefer, H. F. *J. Phys. Chem. A* **2001**, *105*, 524−528. (c) Hay, P. J. *J. Phys. Chem. A* **2002**, *106*, 1634−1641. (d) D'Souza, F.; Zandler, M. E.; Smith, P. M.; Deviprasad, G. R.; Arkady, K.; Fujitsuka, M.; Ito, O. *J. Phys. Chem. A* **2002**, *106*, 649. (e) Zandler, M. E.; Smith, P. M.; Fujitsuka, M.; Ito, O.; D'Souza, F. *J. Org. Chem.* **2002**, *67*, 9122. (f) Marczak, R.; Hoang, V. T.; Noworyta, K.; Zandler, M. E.; Kutner, W.; D'Souza, F. *J. Mater. Chem.* **2002**, *12*, 2123. (g) D'Souza, F.; Deviprasad, G. R.; Zandler, M. E.; El-Khouly, M. E.; Fujitsuka, M.; Ito, O. *J. Phys. Chem. A* **2003**, *107*, 4801.

Table 1. Free-Energy Changes (in eV) for Singlet Energy Transfer ($\Delta G_{ENT}^{singlet}$), Charge Separation ($\Delta G_{CS}^{singlet}$), and Charge Recombination (ΔG_{CR}) for the Dyad and Supramolecular Triad in *o*-Dichlorobenzene

compound	$\Delta G_{ENT}^{singlet,a}$ (ZnP–BDP*)	$\Delta G_{CS}^{singlet,b}$ (ZnP*–BDP)	ΔG_{CR}^{c} (ZnP^{·+}–BDP^{·–})	$\Delta G_{CS}^{singlet,b}$ (C$_{60}$Im–ZnP*–BDP)	ΔG_{CR}^{c} (C$_{60}$Im^{·–}–ZnP^{·+}–BDP)
ZnP–BDP^d	−0.34	−0.50	−1.50		
C$_{60}$Im–ZnP–B DP^e					
expanded	−0.34	−0.57	−1.51	−0.80	−1.28
closed	−0.34	−0.60	−1.48	−0.81	−1.27

a The $\Delta G_{ENT}^{singlet}$ value is the energy difference between the excited singlet state of boron dipyrrin (abbreviated as ^{1}BDP*) and that of ^{1}ZnP* as evaluated from the fluorescence peaks. *b* The ΔG_{CS}^S values are calculated from the Weller equation (ref 25) ($\Delta G_{CS}^S = E_{ox}(ZnP) - E_{red}(A) - E_0 - E_c$), employing the E_0-energy level of ^{1}ZnP* (=2.08 eV) and E_{ox} (ZnP) shown in the text. E_{red}(A) are the reduction potentials of the electron acceptors. E_c(Coulomb energy) was calculated by $(e^2/(4\pi\epsilon_0))[(1/(2R_+) + 1/(2R_-) - 1/R_{cc})/\epsilon_S]$, where R_+ and R_- and R_{cc} are the radii of the cation and anion, and the center-to-center distance between the donor and acceptor, respectively. ϵ_S is the dielectric constant of solvents used for photophysical studies and for measuring the redox potentials. *c* $-\Delta G_{CR} = -E_{ox} + E_{red} - E_c$. *d* Represents the covalently linked ZnP–BDP dyad. *e* Represents the supramolecular triad formed by the addition of 5 equiv of imidazole-appended fulleropyrrolidine (C$_{60}$Im) to the solution of ZnP–BDP dyad.
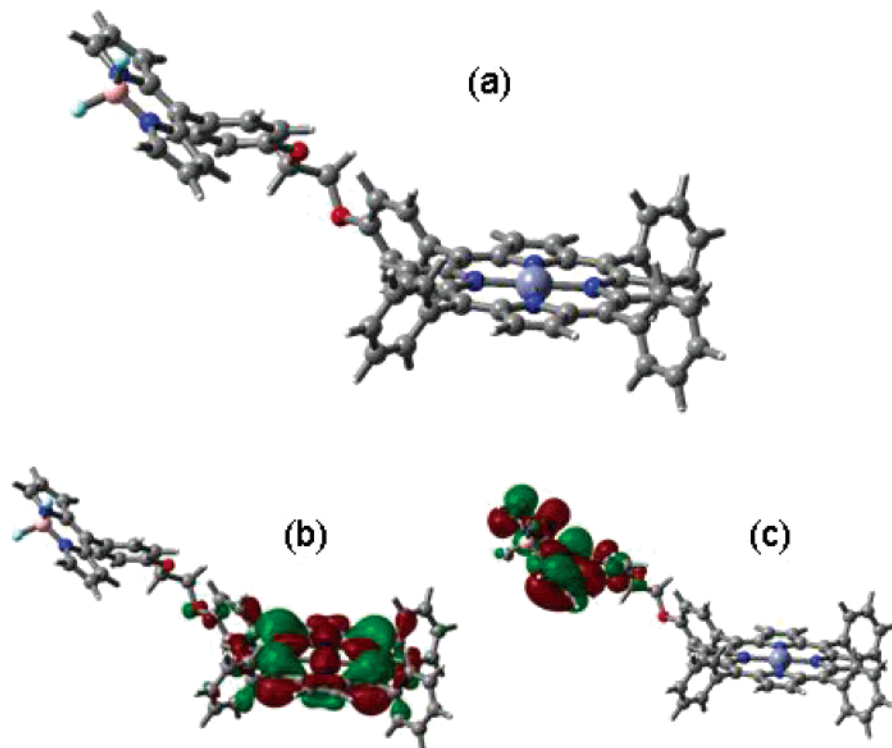
Figure 3. B3LYP/3-21G(*) calculated structure and molecular orbitals for the ZnP–BDP dyad: (a) optimized structure, (b) HOMO, and (c) LUMO.

As shown in Figure 3a, in the optimized structure of the boron dipyrrin–zinc porphyrin dyad, the center-to-center distance (zinc to boron) was found to be ∼12 Å with no steric constraint between the two moieties. Both the porphyrin ring and the dipyrrin ring are planar without significant structural distortions. The computed HOMO and LUMO are both π-orbitals; the former is located on the porphyrin ring, while the latter is located on boron dipyrrin (Figure 3b and c). The location of the LUMO on the boron dipyrrin moiety is consistent with the electrochemical results where the possibility of boron dipyrrin as an electron acceptor is revealed. Because of these observations, in the present study, we have explored the possibilities of boron dipyrrin acting as an electron acceptor from the singlet excited zinc porphyrin in addition to being an excited-state energy donor to the zinc porphyrin, as shown in Scheme 2. The present dyad is especially suitable to probe such events, because of the wavelength selectivity; that is, the ZnP can be selectively excited at 550 nm in the dyad, while the boron dipyrrin can be selectively excited at 388 or 500 nm.

Scheme 2
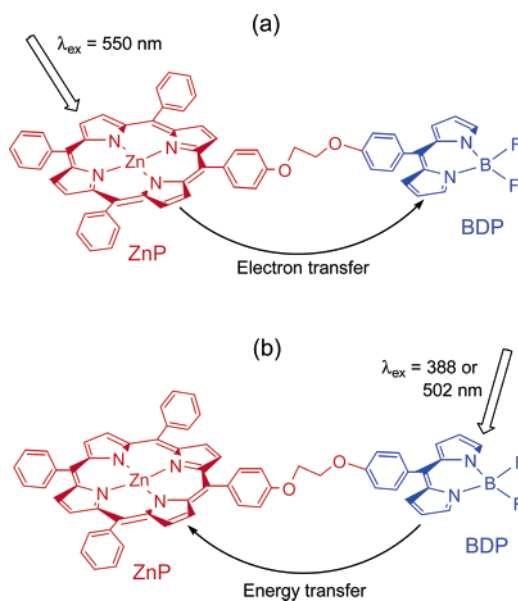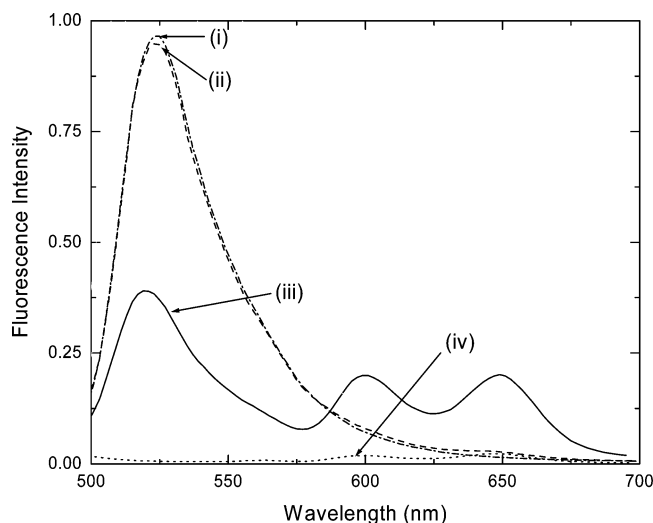
Figure 4. Steady-state fluorescence spectra of (i) BDP, (ii) equimolar amounts of ZnP and BDP, (iii) ZnP−BDP dyad, and (iv) ZnP in *o*-dichlorobenzene. The concentrations were held constant to 0.4 μM for all of the species. λ_{ex} = 502 nm.

Energy Transfer from Singlet Excited Boron Dipyrrin to Zinc Porphyrin in the Dyad. Figure 4 shows the steady-state fluorescence emission spectrum of the dyad along with the control experiments performed to prove the occurrence of energy transfer. At the excitation wavelength of 502 nm, the dyad revealed emission bands at 522 nm corresponding to the emission of the boron dipyrrin moiety, and at 600 and 649 nm corresponding to the emission of the zinc porphyrin moiety (spectrum iii). The emission intensity of the 520 nm band is found to be quenched over 60% as compared to free boron dipyrrin in a control experiment (spectrum i). The presence of equimolar amounts of ZnP in the boron dipyrrin solution had no effect on the emission intensity of boron dipyrrin (spectrum ii), and extending the emission scan to the porphyrin emission region revealed no emission corresponding to ZnP, suggesting no energy transfer from the excited boron dipyrrin under intermolecular conditions. In a separate experiment, when only ZnP was excited at 502 nm, very weak emission of ZnP at 600 and 650 nm (spectrum iv) was observed. This suggests that irradiation of the dyad at 500 nm would not excite the ZnP simultaneously; this observation agrees with earlier reported studies.[22] These control experiments and the diminished emission intensity of the boron dipyrrin moiety and the occurrence of new emission bands corresponding to the zinc porphyrin emission in the dyad clearly indicate the occurrence of photoinduced energy transfer.

Further, the excitation spectrum of the dyad was recorded by monitoring the emission at 650 nm corresponding to ZnP. The spectrum thus recorded was similar to the absorption spectrum of the dyad (see Supporting Information). Control experiments involving ZnP, and equimolar ZnP and boron dipyrrin, revealed an excitation spectrum corresponding to only ZnP. These results provide further evidence for the energy transfer, and the similarity between the absorption and excitation spectrum of the dyad also suggests the occurrence of efficient energy transfer.

To probe the kinetics of energy transfer from excited boron dipyrrin to zinc porphyrin, time-resolved emission spectral studies were performed. When the boron dipyrrin moiety of the
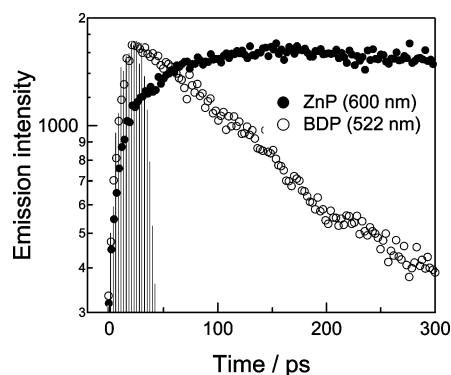
Figure 5. Time resolved fluorescence rise time-profile at 600 nm and decay time-profile at 522 nm, respectively, for ZnP and BDP of the ZnP−BDP dyad in *o*-dichlorobenzene. The sample was excited at 388 nm, and the hatched area shows the pulse profile.

Table 2. Time-Resolved Fluorescence Lifetimes of Investigated Compounds in *o*-Dichlorobenzene

	emission lifetime, τ_F/ps (fraction %)	
compound	BDP[a]	ZnP[b]
ZnP		1920 (100%)
BDP	530 (100%)	
ZnP−BDP	90 (90%)	1200 (100%)
C$_{60}$Im−ZnP−BDP	95 (91%)	1300 (66%), 190 (34%)

[a] λ_{ex} for BDP = 388 nm. [b] λ_{ex} for ZnP = 532 nm.

dyad was excited at a wavelength of 388 nm, the time-profiles for the decay of the boron dipyrrin moiety at 522 nm and the rise of the zinc porphyrin moiety at 600 nm were observed as shown in Figure 5. The data shown in Figure 5 clearly demonstrate the occurrence of the photoinduced energy-transfer process. In *o*-dichlorobenzene, both free boron dipyrrin and ZnP moieties revealed monoexponential decay. The calculated lifetimes were found to be 530 and 1920 ps, respectively, for the free boron dipyrrin and ZnP moieties (Table 2). In the dyad, the decay of the excited boron dipyrrin could also be fitted satisfactorily to monoexponential decay. The decay is attributed to the energy-transfer process, and the calculated rate of energy transfer and quantum yield are listed in Table 3. The rate constant (9.2 × 10^9 s^{-1}) and quantum yield (0.83) indicate efficient energy transfer from the excited boron dipyrrin to zinc porphyrin in the dyad; this observation readily parallels that of the steady-state emission and excitation spectral behavior of the dyad. The energy transfer was also monitored by picosecond transient absorption methods (see Supporting Information), which revealed the emission of ZnP upon excitation of the boron dipyrrin moiety of the dyad.

Electron Transfer from Singlet Excited Zinc Porphyrin to Boron Dipyrrin in the Dyad. As revealed by the electrochemical and computational studies, upon excitation of the zinc porphyrin moiety, electron transfer to the appended boron dipyrrin entity is expected to occur. Steady-state fluorescence results shown in Figure 6 revealed quenching of zinc porphyrin in the dyad over 40% as compared to that of free ZnP at equal concentrations. Time-resolved emission studies also revealed quenching; that is, the decay of excited zinc porphyrin followed a monoexponential decay with a lifetime of 1200 ps (Table 2). The calculated rate of electron transfer and the quantum yield were found to be 3.1 × 10^8 s^{-1} and 0.38, respectively (Table 3). The relatively low rate and quantum yield are expected

Table 3. Singlet Energy-Transfer Rate Constants ($k_{ENT}^{singlet}$), Energy-Transfer Efficiency ($\Phi_{ENT}^{singlet}$), Charge-Separation Rate Constants ($k_{CS}^{singlet}$), and Charge-Separation Quantum Yields ($\Phi_{CS}^{singlet}$) for the Dyad and Supramolecular Triad in o-Dichlorobenzene
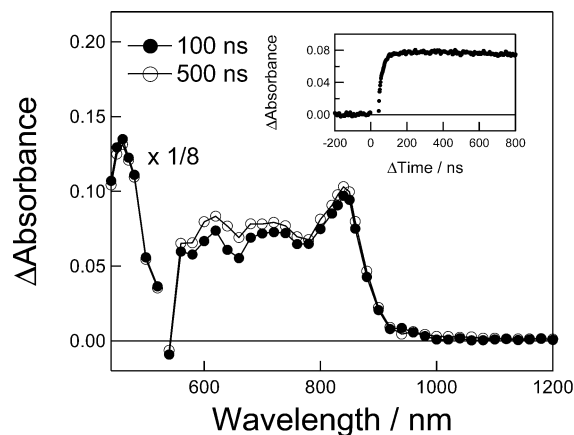
compound	(ZnP–B DP*)[a]		(ZnP*–B DP)[b]		(C_{60}Im–Z nP*)[c]		
	$k_{ENT}^{singlet}$ s$^{-1,a}$	$\Phi_{ENT}^{singlet,a}$	$k_{CS}^{singlet}$ s$^{-1,b}$	$\Phi_{CS}^{singlet,b}$	$k_{CS}^{singlet}$ s$^{-1,c}$	$\Phi_{CS}^{singlet,c}$	k_{CR} s$^{-1,d}$
ZnP–BDP	9.2×10^9	0.83	3.1×10^{8e}	0.38^e			
C_{60}Im–ZnP–BDP	8.6×10^9	0.82	2.5×10^{8f}	$(0.21)^f$	4.7×10^{9g}	$(0.34)^g$	2.0×10^8

^{a} Energy transfer from BDP* to ZnP. Calculated by the following equations: $k_{ENT}^{singlet} = \tau_{F,ZnP-BDP*}^{-1} - \tau_{F,BDP*}^{-1}$ and $\Phi_{ENT}^{singlet} = (\tau_{F,ZnP-BDP*}^{-1} - \tau_{F,BDP*}^{-1})/\tau_{F,ZnP-BDP*}^{-1}$. ^{b} Charge separation between ZnP* and BDP. ^{c} Charge separation between ZnP* and C_{60}Im. ^{d} From the fast decay part at 1000 nm in the nanosecond transient absorption measurement. ^{e} Calculated by the following equations: $k_{CS}^{singlet} = \tau_{F,ZnP*-BDP}^{-1} - \tau_{F,ZnP*}^{-1}$ and $\Phi_{CS}^{singlet} = (\tau_{F,ZnP*-BDP}^{-1} - \tau_{F,ZnP*}^{-1})/\tau_{F,ZnP*-BDP}^{-1}$. ^{f} Calculated from the slow decay part of ZnP* by the following equations: $k_{CS}^{singlet} = \tau_{F,C60Im-ZnP*-BDP}^{-1} - \tau_{F,ZnP*}^{-1}$ and $\Phi_{CS}^{singlet} = (\tau_{F,C60Im-ZnP*-BDP}^{-1} - \tau_{F,ZnP*}^{-1})/\tau_{F,ZnP*-BDP}^{-1}$ after multiplying the fraction. ^{g} Calculated from fast decay part of ZnP* by equations in footnote f.
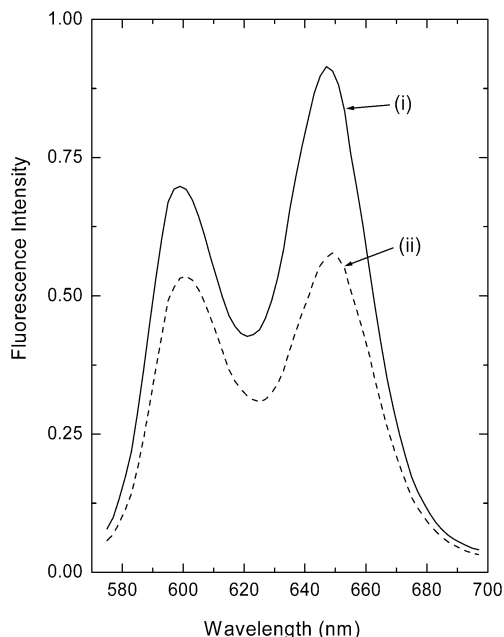
Figure 6. Steady-state fluorescence spectra of (i) ZnP (2.4 μM) and (ii) ZnP–BDP dyad (2.4 μM) in o-dichlorobenzene. λ_{ex} = 550 nm.

Figure 7. Transient absorption spectra of the ZnP–BDP dyad (0.05 mM) at 100 ns (●) and 500 ns (○) after the 550 nm laser irradiation in Ar-saturated o-dichlorobenzene. Inset: Absorption–time-profiles at 625 nm in Ar-saturated o-dichlorobenzene.

because of the low ΔG_{CS} (−0.57 to −0.60 eV) associated with the electron transfer via ^{1}ZnP* in the dyad.

Further transient absorption studies were performed to characterize the electron-transfer products. Spectroelectrochemical studies were also performed to characterize the one-electron reduced product of boron dipyrrin. During the electrolysis, no new absorption bands corresponding to the boron dipyrrin anion radical were observed in the wavelength region scanned until 1000 nm; however, the 500 nm band of neutral boron dipyrrin revealed a considerable decrease in intensity (see Supporting Information). The nanosecond transient absorption spectra using 550 nm laser light recorded for the dyad are shown in Figure 7. Intense absorption at 460 nm and a band at 700–850 nm corresponding to the triplet state of zinc porphyrin (^{3}ZnP*) were observed. In a control experiment, the transient absorption spectrum recorded for boron dipyrrin revealed no specific peak corresponding to its triplet state (see Supporting Information). In the absence of characteristic bands for the boron dipyrrin anion radical, it was, however, difficult to spectrally characterize the electron-transfer products. It may be noted here that in the transient absorption spectrum of the dyad, the absorption intensity at 625 nm relative to that of 850 nm seems to be larger than that of ZnP alone (see Supporting Information), suggesting the 625 nm band can be attributed to the cation radical of the ZnP moiety (ZnP$^{•+}$) in the dyad, which may be overlapping with the absorption tail of the ^{3}ZnP* moiety at 850 nm. The

time-profile at 625 nm shown in the inset of Figure 7 revealed that the ZnP$^{•+}$ moiety rises relatively quickly, although the initial rise profile is hidden by the depletion or fluorescence of the ZnP moiety. The decay at 625 nm is slow without showing a rapid decay component, which suggests the generation of a relatively long-lived charge-separated state in o-dichlorobenzene. However, we could not perform further analysis of the data due to the overlapping of the ZnP$^{+•}$ band with the ^{3}ZnP* absorption band in this wavelength region.

Formation of the Boron Dipyrrin–Zinc Porphyrin–Fullerene Supramolecular Triad. The formation of the supramolecular triad was followed by optical absorption spectral methods. Figure 8 shows the spectral changes observed during the addition of imidazole-appended fulleropyrrolidine to the ZnP–BDP dyad in o-dichlorobenzene. The Soret band at 425 nm first decreased in intensity and then increased with a red shift to 432 nm. Isosbestic points at 418 and 429 nm were observed, indicating the occurrence of an equilibrium process in solution. It may be mentioned here that the band at 502 nm corresponding to the boron dipyrrin moiety revealed no peak shift during the course of the titration, indicating no significant interactions with the fullerene; the increase in the absorbance at 502 nm is attributed to the absorption of added imidazole bearing fulleropyrrolidine. Independent control experiments performed in the presence of boron dipyrrin and imidazole functionalized fullerene also revealed no spectral changes. These results suggest that only the zinc porphyrin is involved in axial coordination and not the boron dipyrrin of the dyad.

The binding constant was evaluated by employing the Scatchard method[29] (Figure 8, inset). The calculated binding constant was found to be 16 500 M^{-1}, which was comparable
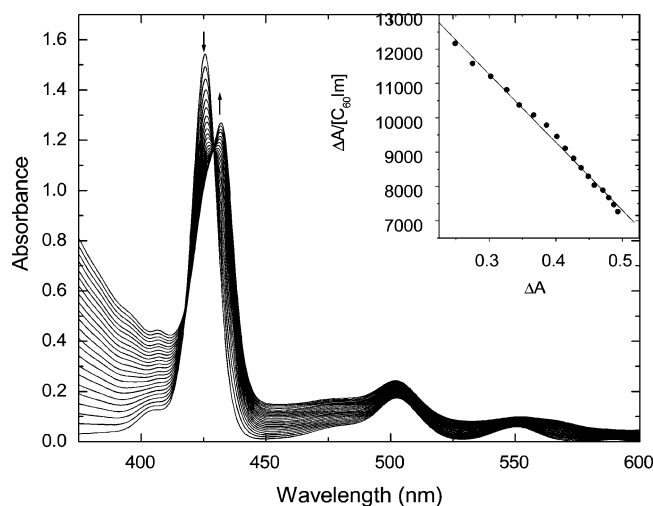
Figure 8. Optical absorption spectral changes observed during the titration of $C_{60}Im$ (3.57 μM each addition) with the ZnP—BDP dyad (2.3 μM) in *o*-dichlorobenzene. The inset figure shows the Scatchard plot of the change of absorbance at 425 nm.

to a binding constant of 16 100 M^{-1} for the same fullerene compound binding to ZnP in *o*-dichlorobenzene. These results indicate stable supramolecular triad formation by the axial ligation approach. The geometric and electronic structure of the triad was also visualized by performing computational studies. Figure 9 shows the optimized structures of the triad in its "closed" and "extended" forms with respect to the boron dipyrrin and C_{60} moieties, at two local minima. It may be mentioned here that due to the flexibility of the supramolecular triad, other intermediate structures were possible; however, the two structures shown in Figure 9a and b can be considered to be the two extreme "closed" and "extended" conformers with little or no steric hindrance between the different moieties. The center-to-center distances between the zinc center of ZnP and the center of C_{60} were found to vary between 12.3 and 13.0 Å, that is, an almost similar distance between the donor and acceptor entities irrespective of their overall geometry. The calculated HOMO and LUMO for the closed and extended structures are shown in Figure 9c, d, e, and f. As predicted from the electrochemical studies, the HOMO was found to be located on the ZnP moiety, while the LUMO was found to be on the fullerene moiety for both of the structures. That is, upon forming the triad, the LUMO moved to the fullerene entity from its original location on the boron dipyrrin moiety in the dyad (see Figure 3).

Energy Transfer Followed by Electron Transfer in the Supramolecular Triad. Figure 10 shows the fluorescence spectra of the ZnP—boron dipyrrin dyad in the presence of increasing amounts of imidazole-appended fulleropyrrolidine at the excitation wavelength of 502 nm corresponding to the excitation of the boron dipyrrin of the dyad. The emission bands corresponding to both boron dipyrrin and zinc porphyrin revealed quenching, without changing the ratio of fluorescence intensity of boron dipyrrin to that of ZnP. The quenching of zinc porphyrin emission in the boron dipyrrin—zinc porphyrin—fullerene triad upon exciting the boron dipyrrin moiety clearly indicates the occurrence of energy transfer from boron dipyrrin to the zinc porphyrin followed by electron-transfer quenching from the singlet excited zinc porphyrin to the coordinated

(29) Scatchard, G. *Ann. N.Y. Acad. Sci.* **1949**, *51*, 661.

fulleropyrrolidine. Further time-resolved emission and transient absorption spectral studies were performed to arrive at the kinetics and characterization of the electron-transfer products.

Figure 11 shows the fluorescence decay profiles for pristine ZnP, the ZnP—BDP dyad, and the supramolecular triad formed by the addition of 5 equiv of imidazole-appended fulleropyrrolidine to the dyad by the excitation of the ZnP moiety. Upon forming the triad, the fluorescence lifetime of the singlet excited zinc porphyrin revealed a biexponential decay with additional quenching as compared to that observed for the dyad alone (Figure 11). Assuming that the additional decay of the excited zinc porphyrin is due to the electron-transfer process to the coordinated fullerene, the rate of electron transfer and quantum yield were calculated. The magnitudes of $k_{CS}^{singlet}$ and $\Phi_{CS}^{singlet}$ in Table 3 reveal efficient electron transfer. The possibility of a competing direct electron transfer from the singlet excited boron dipyrrin to the fulleropyrrolidine was considered to be a minor route even though one of the optimized geometries in Figure 9 showed close proximity of boron dipyrrin and C_{60}. This is because the calculated free-energy change for this process was found to be weakly exothermic ($\Delta G = \sim -0.17$ eV) as compared to the highly exothermic electron transfer from the singlet excited ZnP to the coordinated C_{60} (Table 1). Moreover, we did not observe additional quenching of the excited lifetime of the boron dipyrrin in ZnP—BDP on addition of imidazole-appended fulleropyrrolidine to form the triad (Tables 2 and 3). To further substantiate this, intermolecular quenching experiments involving phenyl boron dipyrrin (50 μM) and 2-phenyl fulleropyrrolidine were performed. In the presence of excess amounts of fulleropyrrolidine (0.5 mM), the quenching of the boron dipyrrin singlet emission was found to be less than 5%. These observations clearly suggest the occurrence of little or no intramolecular electron transfer from the excited boron dipyrrin to the fullerene in the supramolecular triad.

Nanosecond transient absorption spectra of the supramolecular triad were recorded to obtain evidence for the energy-transfer followed by electron-transfer mechanism. Figure 12 shows the transient absorption spectra, upon forming the triad by the addition of 5 equiv of imidazole-appended fulleropyrrolidine to the dyad in *o*-dichlorobenzene, after the 500 nm laser irradiation to generate ^{1}BDP*. Transient absorption bands corresponding to the triplet excited zinc porphyrin and fullerene were observed at 850 and 700 nm. In addition, a band at 1000 nm was observed corresponding to the fulleropyrrolidine anion radical formation. The inset figure shows the time-profile of this peak which exhibits an immediate rise and decay, indicating that the signal arises from the charge-separation process, via the singlet excited zinc porphyrin, which is produced by energy transfer from the singlet excited state of the boron dipyrrin entity. From the decay rate, the charge-recombination rate constant (k_{CR}) was evaluated to be 2.0×10^8 s^{-1} in *o*-dichlorobenzene as seen in the inset time-profile of Figure 12. The slower decay part could be attributed either to the absorption tail of the ^{3}ZnP* moiety at 860 nm or to the possible occurrence of bimolecular back electron transfer between free radical ions produced by the dissociation of the charge-separated state, under the conditions when the dissociation of the charge-separated state competes with intramolecular charge recombination.
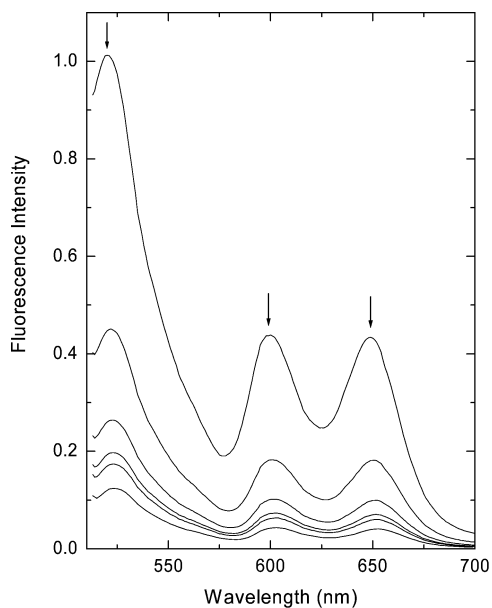
Energy Level Diagram. The results of the present investigation along with all of the control experiments clearly show the
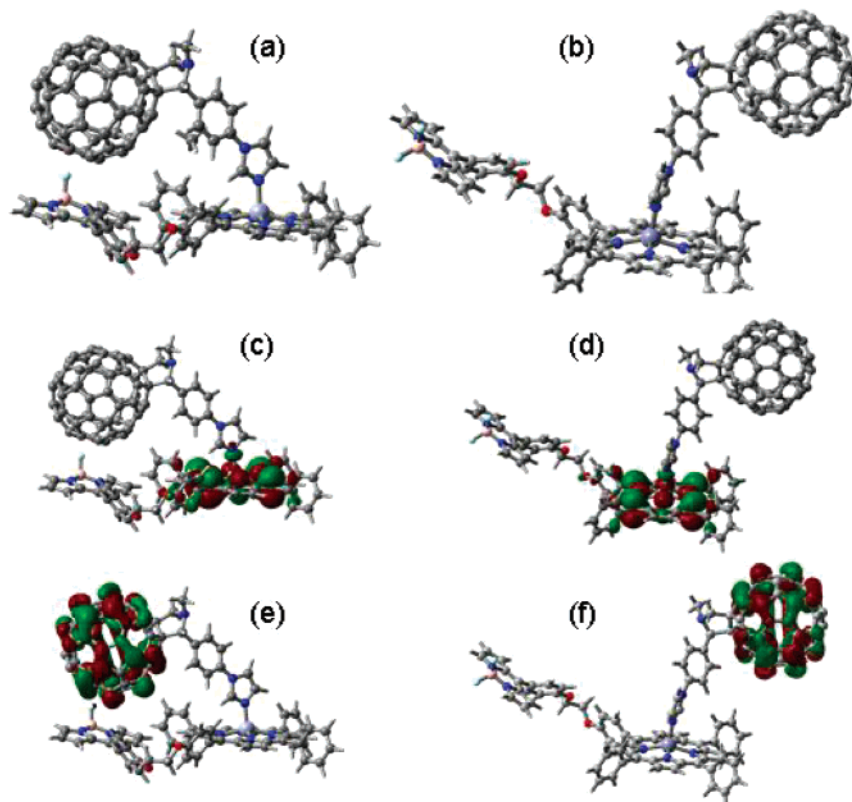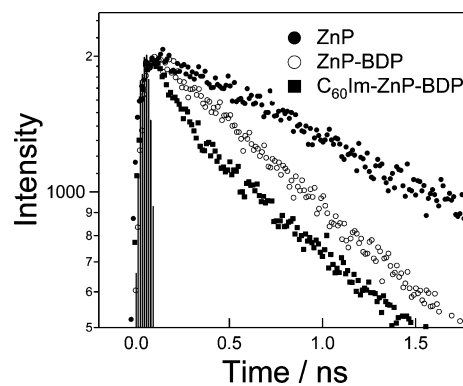
Figure 9. B3LYP/3-21G(*) optimized structure at local minima for the supramolecular triad formed by coordinating $C_{60}Im$ to ZnP−BDP in (a) "closed" and (b) "extended" forms. The corresponding HOMO and LUMO are shown in parts c, d, e, and f.

Figure 10. Steady-state fluorescence spectrum of the ZnP−BDP dyad (1.75 μM) in the presence of increasing amounts of $C_{60}Im$ (2.0 μM each addition) in *o*-dichlorobenzene. $\lambda_{ex} = 502$ nm.

Figure 11. Fluorescence decay time-profiles at 600 nm of (a) ZnP, (b) ZnP−BDP dyad, and (c) the supramolecular triad formed by coordinating $C_{60}Im$ to the ZnP−BDP dyad in *o*-dichlorobenzene. The samples were excited at 550 nm, and the hatched area shows the pulse profile.

occurrence of efficient energy transfer followed by electron transfer in the studied supramolecular triad, although the photochemistry of the multichromophoric triad seems to be fairly complex. The combination of optical absorption, steady-state fluorescence emission, molecular modeling, electrochemistry, and time-resolved emission and transient absorption studies has permitted the extraction of the needed energetic and kinetic information. The different photochemical events observed in

the triad are depicted in Figure 13 in the energy level diagram. Energies of the excited states of the different entities were calculated from the fluorescence peaks, while the triplet state energy of ZnP was cited from the literature.[31] The driving forces for the occurrence of electron transfer from the different excited chromophores of the triad are cited from Table 1. In the energy level diagram, the thick arrows indicate the major process, and the dotted arrows are the minor process. In the case of the dyad, although charge separation occurs from $^{1}ZnP^{*}$, generating $ZnP^{•+}$ and $BDP^{•−}$, this process seems to be incompetent in the triad. That is, upon excitation of BDP in the triad, the major process

(30) D'Souza, F.; Deviprasad, G. R.; El-Khouly, M. E.; Fujitsuka, M.; Ito, O. *J. Am. Chem. Soc.* **2001**, *123*, 5277.
(31) Smith, K. M. *Porphyrins and Metalloporphyrins*; Elsevier: New York, 1977.
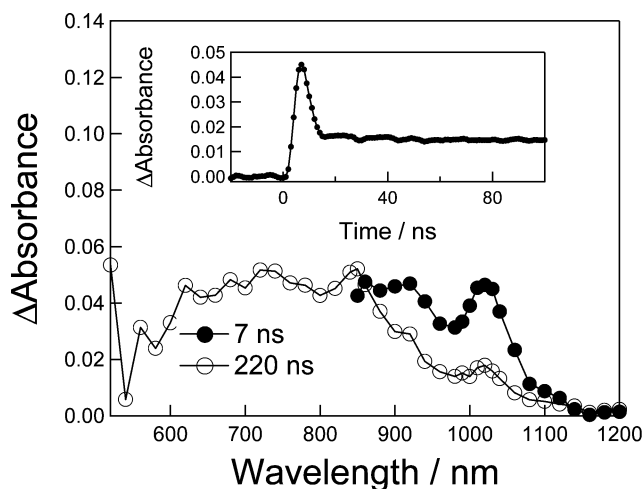
Figure 12. Transient absorption spectra of the supramolecular triad formed by mixing $C_{60}Im$ (0.25 mM) and ZnP–BDP (0.05 mM) in *o*-dichlorobenzene at 7 ns (●) and 160 ns (○) after the 500 nm laser irradiation. Inset: Absorption–time-profiles at 1020 nm.
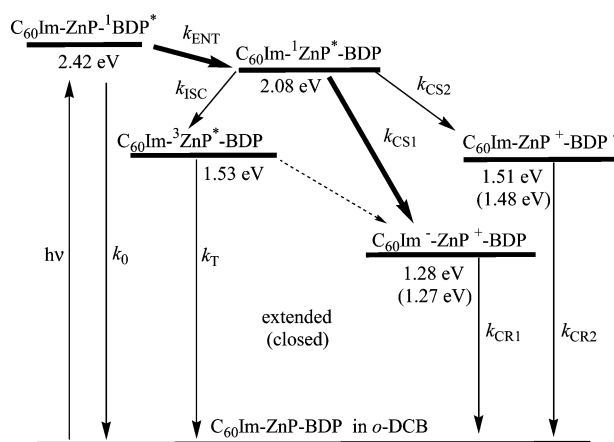
Figure 13. Energy level diagram showing the different photochemical events of the supramolecular $C_{60}Im$–ZnP–BDP triad after excitation of the BDP moiety; numbers in parentheses are for the "closed" structure.

involves charge separation to form $C_{60}Im^{\cdot-}$–$ZnP^{\cdot+}$–BDP because of the appropriate exothermic conditions.

Conclusions

A supramolecular triad constructed via axially coordinating imidazole-appended fulleropyrrolidine to the zinc center of a covalently linked zinc porphyrin–boron dipyrrin dyad was successfully shown to be a model of the photosynthetic antenna-reaction center complex. Efficient energy transfer from the singlet excited boron dipyrrin to the zinc porphyrin as well as electron transfer from the singlet excited zinc porphyrin to the boron dipyrrin entity was observed in the dyad. As revealed by the steady-state and time-resolved emission as well as transient absorption spectral studies, in the supramolecular triad, the boron dipyrrin absorbs light energy and transfers it to the zinc porphyrin to create the singlet excited zinc porphyrin. Electron transfer from the excited zinc porphyrin to fullerene subsequently follows, resulting in the formation of the charge-separated state. The observed energy transfer followed by electron transfer in the studied supramolecular triad mimics successfully the "combined antenna-reaction center" events of natural photosynthesis. ■

Experimental Section

Chemicals. Buckminsterfullerene, C_{60} (+99.95%), was from SES Research (Houston, TX). *o*-Dichlorobenzene in a sure seal bottle, sarcosine, pyrrole, trifluoroacetic acid (TFA), dichlorodicyanobenzoquinone (DDQ), triethylamine, and benzaldehyde derivatives (benzaldehyde, 4-bromoethoxybenzaldehyde, 4-imidazolyl benzaldehyde, and *o*- and *p*-hydroxy benzaldehyde) were from Aldrich Chemicals (Milwaukee, WI). Tetra-*n*-butylammonium perchlorate, (TBA)ClO$_4$, was from Fluka Chemicals. All of the chromatographic materials and solvents were procured from Fisher Scientific and were used as received. Syntheses and purification of imidazole-appended fulleropyrrolidine,[24] 5-(4-hydroxyphenyl)-10,15,20-triphenylporphyrin, free-base and zinc porphyrins, H$_2$P and ZnP, and *meso*-phenyl boron dipyrrin were carried out according to the literature procedures.[30–32]

***meso*-[4-(Bromoethoxy)phenyl]dipyrromethane (1).** This was synthesized according to the general procedure developed by Lindsey for boron dipyrrin synthesis.[32] To a solution of argon-purged bromoethoxybenzaldehyde (300 mg, 1.0 mmol) and pyrrole (3.63 mL, 52.4 mmol) was added TFA (10 µL, 0.01 mmol), and the mixture was stirred for 15 min. The reaction mixture was diluted with CH$_2$Cl$_2$ and quenched with 0.1 M NaOH (50 mL), and then washed with water and dried over sodium sulfate. The solvent and excess pyrrole were then vacuum distilled at room temperature. The compound was purified over silica gel flash column using cyclohexane/ethyl acetate (70:30 v/v) as eluent. Yield 250 mg. ^{1}H NMR (CDCl$_3$): δ ppm, 7.79 (s br, 2H), 7.08 (d, 2H), 6.82 (d, 2H), 6.60 (m, 2H), 6.12 (m, 2H), 5.85 (s, 2H), 5.33 (s, 1H), 4.21 (t, 2H), 3.57 (t, 2H). ESI mass in CH$_2$Cl$_2$ calcd, 329.3; found, 329.5.

N,N′-Difluoroboryl-5-[4-(bromoethoxy)phenyl]dipyrrin (2). To a solution of **1** (500 mg, 1.5 mmol) dissolved in dry toluene (30 mL) was added DDQ (345 mg, 1.5 mmol), and the mixture was stirred for 15 min. Triethylamine (1.48 mL, 10.6 mmol) was then added, followed immediately by BF$_3$-etherate (1.34 mL, 10.6 mmol), and the mixture was stirred for another 30 min. The reaction mixture was washed with water and dried over sodium sulfate. The compound was purified over silica gel column using CH$_2$Cl$_2$/hexanes (2:1 v/v) as eluent. The solvent was evaporated under reduced pressure, and the resulting orange solid was washed repeatedly with hexanes. Yield 190 mg. ^{1}H NMR (CDCl$_3$): δ ppm, 7.93 (s, 2H), 7.56 (d, 2H), 7.07 (d, 2H), 6.96 (m, 2H), 6.56 (m, 2H), 4.40 (t, 2H), 3.71 (t, 2H). UV–vis in *o*-dichlorobenzene, λ_{max} nm, 502. ESI mass in CH$_2$Cl$_2$ calcd, 391.0; found, 392.1.

5-[4-Phenoxyethyl(N,N′-difluoroboryl-5-(4-oxyphenyl)dipyrrin)]-10,15,20-triphenylporphyrin (3). To a solution of **2** (74 mg, 0.19 mmol) and 5-(4-hydroxyphenyl)-10,15,20-triphenylporphyrin (40 mg, 0.06 mmol) dissolved in DMF (30 mL) was added an excess of potassium carbonate, and the mixture was stirred for 18 h. The mixture was suction filtrated, and the solvent was evaporated under reduced pressure. The product was purified over silica gel column using CHCl$_3$/hexanes (40:60 v/v) as eluent. Yield 25 mg. ^{1}H NMR (CDCl$_3$): δ ppm, 8.83–8.89 (m, 8H), 8.20–8.24 (m, 6H), 8.16 (d, 2H), 7.95 (s, 2H), 7.73–7.79 (m, 9H), 7.63 (d, 2H), 7.36 (d, 2H), 7.23 (d, 2H), 7.03 (m, 2H), 6.57 (m, 2H), 4.68 (m, 2H), 4.62 (m, 2H), −2.77 (s br, 2H). UV–vis in *o*-dichlorobenzene, λ_{max} nm, 423, 503, 552, 593. ESI mass in CH$_2$Cl$_2$ calcd, 940.3; found, 941.5.

5-[4-Phenoxyethyl(N,N′-difluoroboryl-5-(4-oxyphenyl)dipyrrin)]-10,15,20-triphenylporphyrinatozinc(II) (4). To a solution of **3** (25 mg, 0.03 mmol) dissolved in chloroform was added zinc acetate (33 mg, 0.15 mmol) dissolved in methanol, and the solution was stirred for 1 h. The solution was washed with water and evaporated under reduced pressure. The compound was purified over silica gel column CHCl$_3$/hexanes (50:50 v/v) as eluent. Yield 27 mg. ^{1}H NMR (CDCl$_3$): δ ppm, 8.93–9.01 (m, 8H), 8.21–8.25 (m, 6H), 8.16 (d, 2H), 7.95 (s, 2H), 7.73–7.80 (m, 9H), 7.64 (d, 2H), 7.35 (d, 2H), 7.23 (d, 2H), 7.03

(32) Wagner, R. W.; Lindsey, J. S. *Pure Appl. Chem.* **1996**, *68*, 1373.

(m, 2H), 6.58 (m, 2H), 4.69 (m, 2H), 4.63 (m, 2H). UV–vis in *o*-dichlorobenzene, λ_{max} nm, 425, 502, 550, 590. ESI mass in CH_2Cl_2 calcd, 1001.6; found, 1002.5.

Instrumentation. The UV–visible spectral measurements were carried out with a Shimadzu model 1600 UV–visible spectrophotometer. The fluorescence emission was monitored with a Spex Fluorolog-tau spectrometer. A right angle detection method was used. The ^{1}H NMR studies were carried out on a Varian 400 MHz spectrometer. Tetramethylsilane (TMS) was used as an internal standard. Cyclic voltammograms were recorded on a EG&G model 263A potentiostat using a three-electrode system. A platinum button electrode was used as the working electrode. A platinum wire served as the counter electrode, and a Ag/AgCl electrode was used as the reference electrode. A ferrocene/ferrocenium redox couple was used as an internal standard. All of the solutions were purged prior to electrochemical and spectral measurements using argon gas. The computational calculations were performed by ab initio B3LYP/3-21G(*) methods with the Gaussian 98[27] software package on various PCs. The graphics of HOMO and LUMO coefficients were generated with the help of GaussView software. The ESI-mass spectral analyses of the newly synthesized compounds were performed with a Fennigan LCQ-Deca mass spectrometer. For this, the compounds (about 0.1 mM concentration) were prepared in CH_2Cl_2, freshly distilled over calcium hydride.

Time-Resolved Emission and Transient Absorption Measurements. The picosecond time-resolved fluorescence spectra were measured using an argon-ion pumped Ti:sapphire laser (Tsunami) and a streak scope (Hamamatsu Photonics). The details of the experimental setup are described elsewhere.[33] Nanosecond transient absorption spectra in the NIR region were measured by means of laser-flash photolysis; 532 nm light from a Nd:YAG laser was used as the exciting source, and a Ge-avalanche-photodiode module was used for detecting the monitoring light from a pulsed Xe-lamp as described in our previous report.[34]

Supporting Information Available: Spectro electrochemistry of boron dipyrrin during the first electroreduction in *o*-dichlorobenzene; excitation spectra of the boron dipyrrin–zinc porphyrin dyad, zinc porphyrin, and boron dipyrrin collected at 650 nm; nanosecond transient absorption spectra of boron dipyrrin in *o*-dichlorobenzene; nanosecond transient absorption spectra of zinc porphyrin and boron dipyrrin–zinc porphyrin in *o*-dichlorobenzene; and the picosecond time-resolved fluorescence emission spectra of the boron dipyrrin–zinc porphyrin in *o*-dichlorobenzene. This material is available free of charge via the Internet at http://pubs.acs.org.

JA030647U

(33) (a) Matsumoto, K.; Fujitsuka, M.; Sato, T.; Onodera, S.; Ito, O. *J. Phys. Chem. B* **2000**, *104*, 11632. (b) Komamine, S.; Fujitsuka, M.; Ito, O.; Morikawa, K.; Miyata, T.; Ohno, T. *J. Phys. Chem. A* **2000**, *104*, 11497. (c) Yamazaki, M.; Araki, Y.; Fujitsuka, M.; Ito, O. *J. Phys. Chem. A* **2001**, *105*, 8615. (d) Fujitsuka, M.; Ito, O.; Yamashiro, T.; Aso, Y.; Otsubo, T. *J. Phys. Chem. A* **2000**, *104*, 4876.

(34) (a) Watanabe, A.; Ito, O. *J. Phys. Chem.* **1994**, *98*, 7736. (b) Ito, O.; Sasaki, Y.; Yoshikawa, Y.; Watanabe, A. *J. Phys. Chem.* **1995**, *99*, 9838. (c) Nojiri, T.; Alam, M. M.; Konami, H.; Watanabe, A.; Ito, O. *J. Phys. Chem. A* **1997**, *101*, 7943.